

Steam Reforming of Toluene as Biomass Tar Model Compound in a Gliding Arc Discharge Reactor

Shiyun Liu, Danhua Mei, Li Wang, Xin Tu*

Department of Electrical Engineering and Electronics, University of Liverpool, Liverpool,
L69 3GJ, UK

Corresponding Author

* Dr. Xin Tu

Department of Electrical Engineering and Electronics,

University of Liverpool,

Liverpool, L69 3GJ,

UK

Tel: +44-1517944513

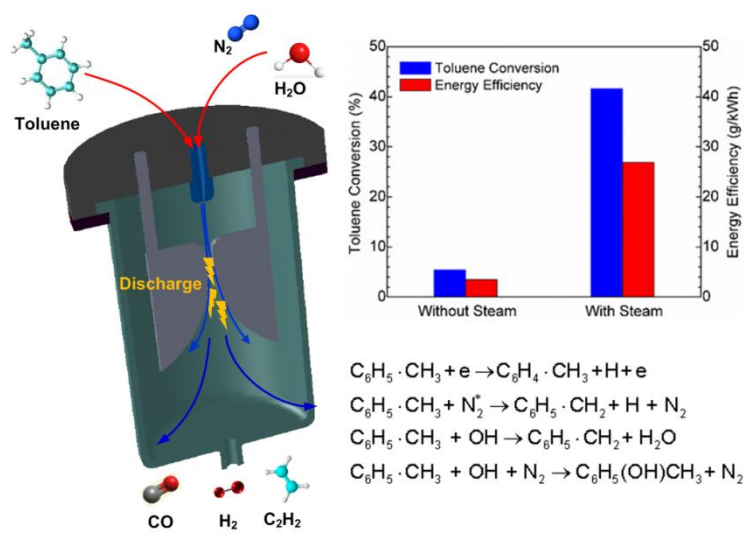
E-mail: xin.tu@liverpool.ac.uk

Abstract

Non-thermal plasma is considered a promising and attractive approach for the removal of tars from biomass gasification to deliver a clean and high quality syngas (a mixture of H₂ and CO). In this study, an AC gliding arc discharge (GAD) reactor has been developed for the conversion of toluene as a tar model compound using nitrogen as a carrier gas. The presence of steam in the plasma reaction produces OH radicals which open a new reaction route for the conversion of toluene through a stepwise oxidation of toluene and intermediates, resulting in a significant enhancement in both the conversion of toluene and the energy efficiency of the plasma process. The effects of steam-to-carbon (S/C) molar ratio, toluene feed rate and specific energy input (SEI) on the performance of the plasma steam reforming of toluene have been investigated. The optimal S/C molar ratio was found to be between 2 and 3 for high toluene conversion and energy efficiency. The maximum toluene conversion of 51.8% was achieved at an optimal S/C molar ratio of 2, a toluene feed flow rate of 4.8 ml/h and a SEI of 0.3 kWh/m³, while the energy efficiency of the plasma process reached a maximum (~46.3 g/kWh) at a toluene feed flow rate of 9.6 ml/h and a SEI of 0.19 kWh/m³. H₂, CO and C₂H₂ were identified as the major gas products with a maximum syngas yield of 73.9% (34.9% for H₂ and 39% for CO). Optical emission spectroscopy has been used to understand the role of steam on the formation of reactive species in the plasma conversion of toluene. The possible reaction pathways in the plasma conversion of toluene have also been proposed by combined means of the analysis of gas and liquid samples and OES diagnostics.

Keywords: Gliding arc discharge; biomass gasification; tar removal; steam reforming of toluene; optical emission spectroscopy

Graphical abstract



1. Introduction

Biomass has been highlighted as a key renewable feedstock to respond to the vital societal need for a step change in the sustainability of energy production which is required to combat climate change. Gasification of biomass wastes represents a major sustainable route to produce syngas (H_2 and CO) from a source which is renewable and CO_2 -neutral [1]. The product gas possesses ease of handling, storability and has great potential for the synthesis of value-added fuels and chemicals. The product gas can also be used in furnaces, boilers, gas engines, gas turbines and fuel cells. However, one of the major challenges in the gasification process is the contamination of the product syngas with tar, particulate matter and other pollutants. Tar is the key problem for biomass gasification and is a complex mixture of condensable hydrocarbons. The tar content of the syngas resulting from the gasification of biomass can range from 1 g/m^3 up to 100 g/m^3 , depending on the gasifier type. The formation of tar causes major process and syngas end-use problems, including tar blockages, plugging and corrosion in downstream fuel lines, filters, engine nozzles and turbines. These problems have resulted in high operational costs and even plant shut-down. It is worth noting that most high efficiency syngas end-use applications such as gas turbines require a low tar content of less than 5 mg/m^3 , orders of magnitude below the tar content in raw syngas. In addition, the tars contain a range of polycyclic aromatic hydrocarbons, some of which have been shown to be carcinogenic. The impact of high tar content in the product gas stream from biomass gasification is a major barrier to the deployment of the technology particularly where very clean gas streams are required such as for high efficiency internal combustion engines and gas turbines and in the future for fuel cells. Therefore, efficient removal of tars from the product gas is crucial in biomass gasification processes [2-4].

Various gas cleaning processes have been proposed for the removal of tars from biomass gasification, including thermal cracking [5, 6], mechanical separation [7, 8] and catalytic reforming [9-11]. Thermal cracking process requires very high temperatures (>800 °C) to decompose tars, incurring a high energy cost. Removal of tars from syngas with a physical separation process will decrease the overall processing efficiency and cause secondary environmental pollution. Catalytic reforming can convert tars into valuable products at relatively lower temperatures (~ 600 °C) compared to thermal cracking process [12]. However, rapid deactivation of the catalysts by sintering, poisoning and carbon deposition due to the complex composition of tars has been a major challenge for industrial applications.

Non-thermal plasma technology provides an attractive and promising alternative to the conventional approaches for the conversion of tars into clean fuels at a relatively low temperature [13, 14]. In non-thermal plasmas, the overall gas temperature can be as low as room temperature, while the electrons are highly energetic with a typical energy of 1-10 eV. As a result, non-thermal plasma can easily break most chemical bonds and overcome the disadvantage of high temperature required by thermal or catalytic processes, and enable thermodynamically unfavourable chemical reactions to occur under ambient conditions [15]. High reaction rate and fast attainment of steady state in a plasma process allows rapid start-up and shutdown of the plasma process compared to other thermal treatment technologies, which significantly reduces the overall energy cost and offers a promising route for clean fuel production [14, 15]. Up until now, very limited work has been focused on the use of a non-thermal plasma gas cleaning process for the removal of tars from the gasification of biomass or waste. Elott et al. developed a microwave plasma torch for the conversion of tars into CO, carbon and H₂ at high temperatures, incurring high energy cost [16]. Nair et al. used a high voltage (80 kV) pulsed corona for the removal of model tar compounds – a mixture of

naphthalene and phenol [17]. However, the energy cost of this plasma cleaning process was still high as 20% of the electrical power generated from biomass gasification was used for the pulsed plasma process. Gliding arc discharge (GAD) has been considered as a transitional plasma and can be generated by applying an electrical field across two or more electrodes in a laminar or turbulent gas flow [18]. A gliding arc system offers high flexibility for working in a wide range of flow rates and elevated power levels (up to several kV) efficiently. It is worth noting that the electron density (10^{23} - 10^{24} m^{-3}) in a gliding arc is close to that of a thermal plasma and is significantly higher than that of other non-thermal plasmas (e.g. DBD and corona) [14]. These distinguishing features result in high energy efficiency of the plasma process for chemical reactions, and have great potential for the removal of tars from biomass gasification [19]. Most previous studies focused on the effect different operating parameters had on the performance of the tar removal process. However, few analysed the by-products and intermediates in the plasma reforming of tar to better understand the underlying reaction pathways and mechanisms in the plasma process.

In this paper, an AC gliding arc plasma gas cleaning system has been developed for the removal of tars from biomass gasification. Toluene has been chosen as a model tar compound since it represents a major stable aromatic product in the tars formed in high temperature biomass gasification processes [20]. N_2 has been used as a carrier gas in the plasma gas cleaning process. The effect of different processing parameters (e.g. steam-to-carbon (S/C) molar ratio, toluene feed rate and specific energy input (SEI)) on the reaction performance (e.g. toluene conversion, yield of products and energy efficiency) has been investigated. Optical emission spectroscopy (OES) has been used to understand the role of steam on the formation of reactive species (e.g. CH, CN, NH and OH) in the plasma chemical reactions. In addition, the possible reaction mechanisms and pathways involved in the plasma conversion

of toluene have been discussed by combined means of OES and the analysis of gas and liquid products.

2. Experimental

2.1 Experimental setup

Fig. 1 shows the schematic diagram of the experimental setup. The gliding arc reactor consisted of two stainless steel semi-ellipsoidal electrodes (60 mm long and 18 mm wide) fixed in an insulating bracket and symmetrically placed on both sides of a gas nozzle with a diameter of 1.5 mm. The shortest electrode gap (electrode throat) was fixed at 2 mm, while the vertical distance between the nozzle exit and electrode throat was 3 mm. N₂ was used as a carrier gas (BOC, zero grade, 99.999% purity) and injected into the GAD reactor with a flow rate of 3.5 l/min. Toluene (C₇H₈, purity >= 99%, Aldrich) with a flow rate of 3.6 - 9.6 ml/h and water (0 - 20 ml/h) were injected into a pipe by high-resolution syringe pumps (KDS Legato,100). As a result, the concentration of toluene can be changed from 9.5 g/Nm³ to 23.4 g/Nm³, which is within the range of tar concentrations from the gasification process using different gasifiers [3]. The mixed stream (toluene with water) was then heated to 160 °C in a copper pipe with an inner diameter of 4 mm (40 cm in length), equipped with a temperature controller system, to generate a steady-state vapour before flowing into the reactor. The plasma reactor was connected to an AC high voltage power supply with a maximum peak to peak voltage of 10 kV and a frequency of 50 Hz. The arc voltage was measured by a high voltage probe (Testec, TT-HVP 15 HF), while the arc current was recorded by a current monitor (Magnetlab, CT-E 0.5-BNC). All the electrical signals were sampled by a four-channel digital oscilloscope (Tektronix, MDO 3024).

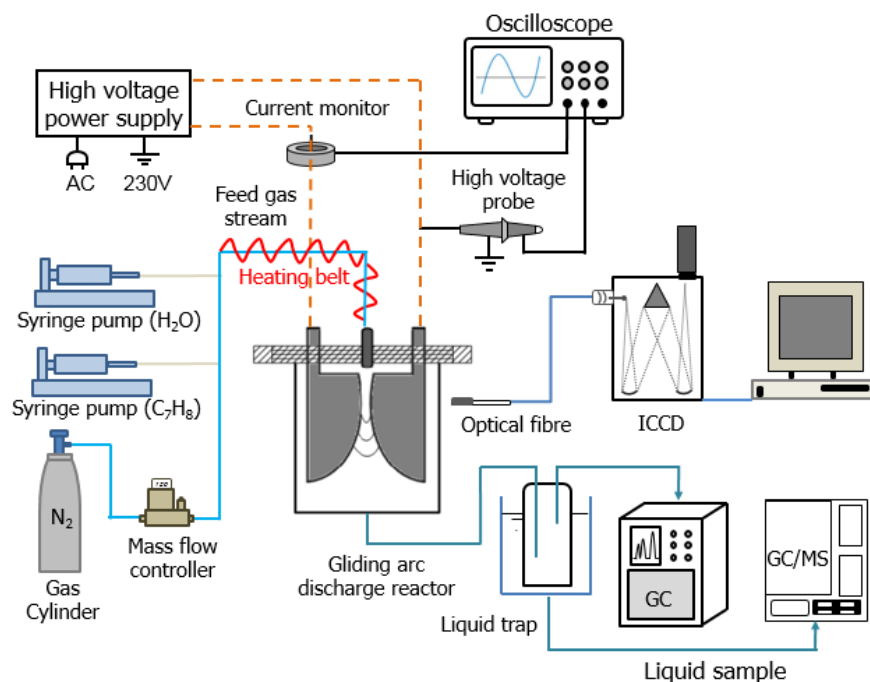


Fig. 1 Schematic diagram of the experimental setup

2.2 Method of analysis and the definition of parameters

The products were sampled when the plasma reaction reached a stable condition. The gaseous products were analyzed by a gas chromatography (Shimadzu, GC-2014) equipped with a thermal conductivity detector (TCD) and a flame ionization detector (FID). A cooling trap was placed at the exit of the plasma reactor to collect the condensable products in the effluent. The collected liquid samples were analyzed by a GC-MS (Agilent GC 7820A, MSD) and qualitatively identified using the mass spectral library from the National Institutes for Standards and Technology (NIST). Emission spectra of the gliding arc discharges under different conditions were recorded by an optical fibre connected to a Princeton Instruments ICCD spectrometer (Model 320 PI) with a focal length of 320 mm.

For the steam reforming of toluene, the discharge power (P) of the plasma process was calculated by the integration of arc voltage and arc current, as shown in Eq. (1).

$$P(W) = \frac{1}{T} \int_0^{t=T} U(t) \times I(t) dt \quad (1)$$

The toluene conversion $X_{C_7H_8}$ was defined as the ratio of the carbon in the carbon-containing gas products (CO, C₂H₂, C₂H₄, C₂H₆ and C₃H₈) to the carbon in the input toluene,

$$X_{C_7H_8} (\%) = \frac{\text{Moles of carbon in the produced gas}}{\text{Moles of carbon in the feed}} \times 100 \quad (2)$$

The yield (Y) of the products can be calculated:

$$Y_{H_2} (\%) = \frac{\text{moles of H}_2 \text{ produced}}{4 \times \text{moles of C}_7\text{H}_8 \text{ input} + \text{moles of H}_2\text{O input}} \times 100 \quad (3)$$

$$Y_{CO} (\%) = \frac{\text{moles of CO produced}}{7 \times \text{moles of C}_7\text{H}_8 \text{ input}} \times 100 \quad (4)$$

$$Y_{C_xH_y} (\%) = \frac{x \times \text{moles of C}_x\text{H}_y \text{ produced}}{7 \times \text{moles of C}_7\text{H}_8 \text{ input}} \times 100 \quad (5)$$

The specific energy input of the discharge was defined as the ratio of the discharge power to the total feed flow rate, as shown in Eq. 6.

$$SEI (\text{kWh/m}^3) = \frac{P (\text{kW})}{\text{Total gas flow rate (m}^3/\text{h)}} \quad (6)$$

The energy efficiency (EE) of the plasma process was determined by the following equation:

$$EE (\text{g/kWh}) = \frac{\text{Converted C}_7\text{H}_8 (\text{g/m}^3)}{SEI (\text{kWh/m}^3)} \quad (7)$$

3. Results and Discussion

3.1 Effect of steam on the plasma conversion of toluene

The plasma conversion of toluene was carried out at a constant toluene flow rate of 4.8 ml/min and a discharge power of 43.5 W with and without steam, as shown in Fig. 2 (a). Clearly, introducing steam into the plasma reaction significantly enhanced the toluene conversion from 5.4 % without steam to 41.6 % with steam, whilst the energy efficiency of

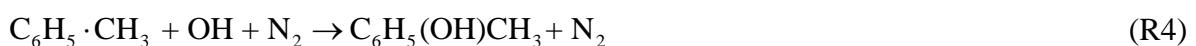
the plasma process was increased by a factor of 8. A similar effect on the plasma chemical reactions from the introduction of water has also been reported in previous studies. Chun et al reported the presence of water promoted the decomposition of benzene in a gliding arc reactor [21]. Yang et al. also found that a humid N₂ plasma exhibited a better performance for the destruction of naphthalene compared to the plasma reaction using dry N₂ as a carrier gas [22].

Adding steam in the N₂ plasma leads to the formation of OH radicals through electron-impact dissociation of H₂O (R1) and collisions of H₂O with N₂ excited species (R2),



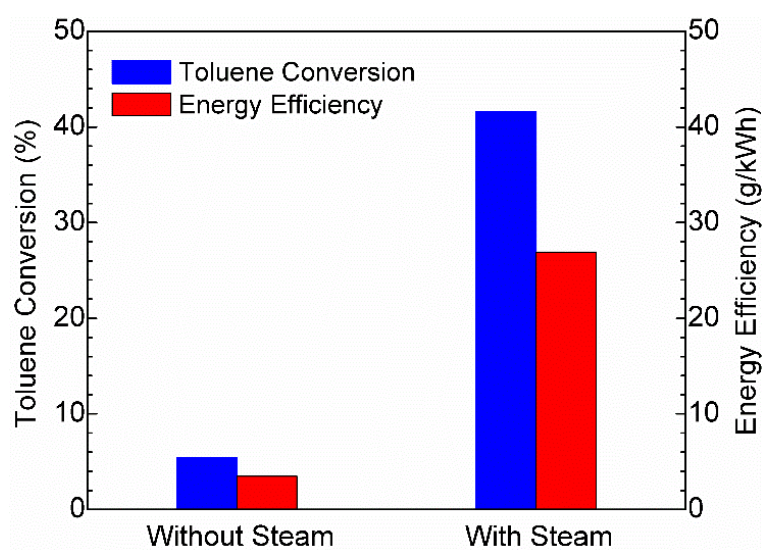
Where N₂^{*} refers to nitrogen excited species N₂ (A³), N₂ (a¹) and N₂ (B).

The generated OH radicals could oxidize toluene (R3 and R4) and intermediates, which provides a new reaction pathway for direct and indirect decomposition of toluene, resulting in a significantly enhanced toluene conversion and energy efficiency compared to the plasma toluene conversion without steam. The formation of OH in the plasma steam reforming of toluene can be confirmed by the presence of OH bands in the spectrum of the N₂/C₇H₈/H₂O GAD (Fig. 3).

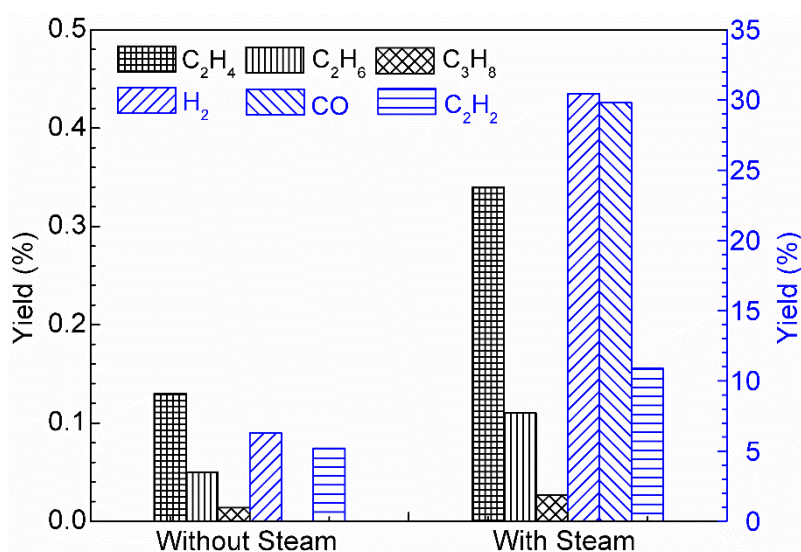


In addition, the presence of steam in the plasma conversion of toluene generated more gas products including H₂, CO, C₂H₆, C₂H₄, C₂H₂ and C₃H₈. For instance, the yield of H₂ (6.3 %) was significantly increased by a factor of 5 when adding steam in this reaction. No CO was

detected in the plasma toluene conversion without steam. However, a high yield of CO (29.8 %) was achieved in the plasma steam reforming of toluene, which suggests that OH might play an important role in the stepwise oxidation reactions, eventually forming CO. It is also interesting to note that no CO₂ was detected in the gas products regardless of whether steam was used in the reaction, while CO₂ is a common by-product in the oxidation of toluene using air plasmas [23].



(a)



(b)

Fig. 2 Effect of steam on (a) toluene conversion and energy efficiency; (b) yields of primary gaseous products (toluene flow rate: 4.8 ml/h; discharge power 43.5 W).

Optical emission spectroscopy was used to investigate the formation of different reactive species in the plasma reforming of toluene with and without steam. Fig. 3 shows the typical spectra of the GAD plasmas using pure N₂, N₂/C₇H₈ and N₂/H₂O/C₇H₈. In the N₂/C₇H₈ plasma without steam, strong CN ($B^2 \Sigma \rightarrow X^2 \Sigma$) violet and second order violet bands can be clearly observed, which might be generated through the following reactions (R5-R7):



The formation of CN might also be linked with carbon deposition in the plasma reaction [24].



The hydrogen Balmer series H_α centred at 653.9 nm and C₂ swan bands in the spectral range of 460-520 nm can also be found, while the intensity of Fulcher band H₂ ($d^3 \Pi_u \rightarrow a^3 \Sigma_g^+$) in the range of 580-650 nm was much weaker compared to that of CN bands.

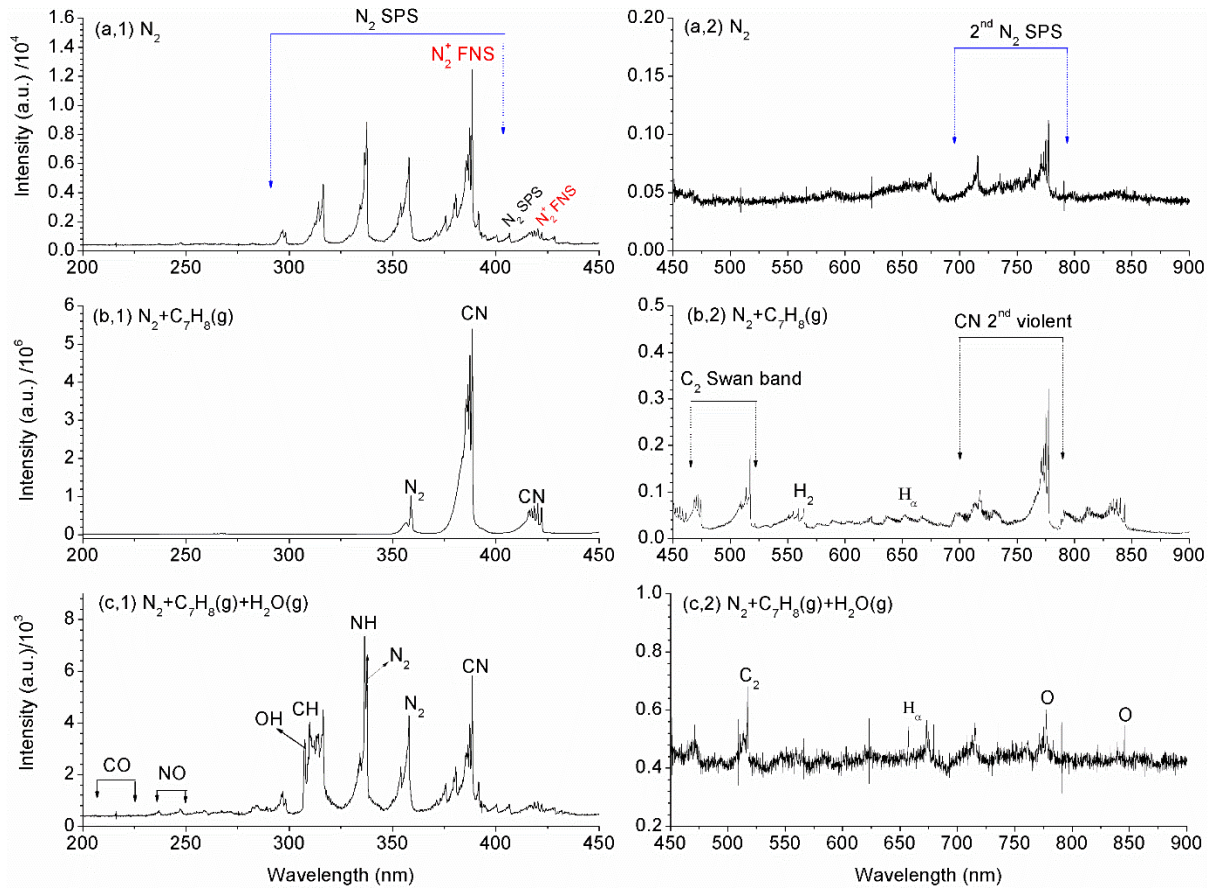


Fig 3. Spectra of optical emission from GAD (a) N_2 GAD plasma; (b) N_2/C_7H_8 GAD plasma; and (c) $N_2/C_7H_8/H_2O$ GAD plasma (C_7H_8 flow rate: 4.8 ml/h; N_2 flow rate: 3.5 l/min; H_2O flow rate: 14.3 ml/h) (600 G/mm grating, exposure time 0.3 s).

Adding steam in the plasma reforming of toluene significantly changed the emission spectrum of the plasma due to the formation of different reactive species in the plasma process. The presence of the OH ($A^2 \Sigma^+ \rightarrow X^2 \Pi$) band in the spectrum of the $N_2/C_7H_8/H_2O$ GAD confirms the dissociation of water through the major reactions R1-R2. Introducing steam into the plasma reforming of toluene significantly reduced the relative intensity of the CN bands but increased the intensity of N_2 ($C^3 \Pi u \rightarrow B^3 \Pi g$) second positive system (350-360 nm). In addition, the spectrum showed a NH ($A^2 \Sigma \rightarrow X^2 \Sigma$) band at 336.1 nm, which could be produced from the reactions of N atoms with H_2O or OH radicals via reactions R9-

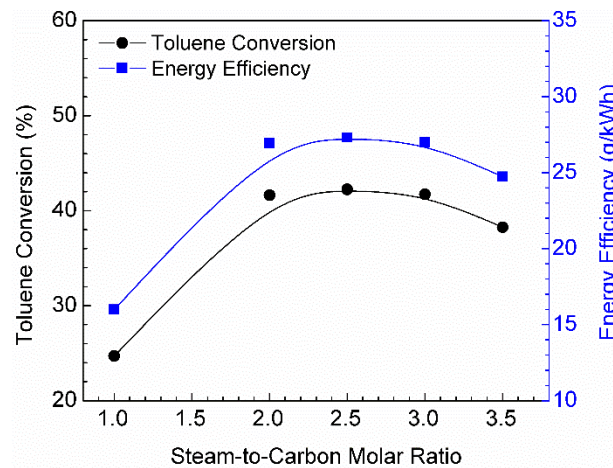
10 as NH band did not appear in the spectrum of the N₂/C₇H₈ plasma without steam [25]. This phenomenon also suggests that the formation of NH via direct reactions between N₂ and H₂ might be ineligible. Moreover, the emissions of CO (A¹Π → X¹Σ) at 200-220 nm and CH (C²Π⁺ → X²Π) at 314.3 nm were also observed. The presence of NO (A²Σ⁺ → X²Π) bands in the range of 230-250 nm suggests that the following reaction might be possible (R11 and R12).



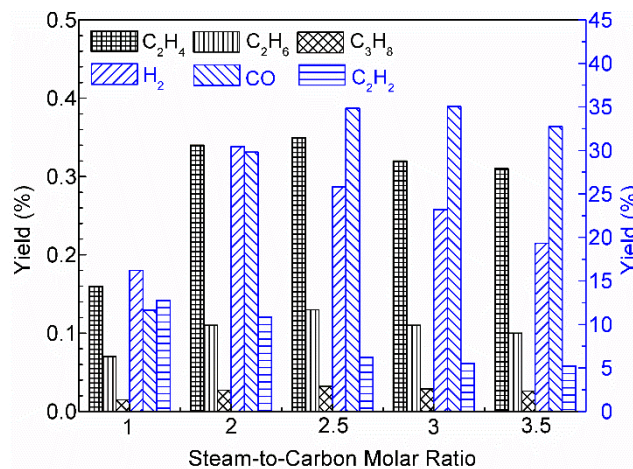
3.2 Effect of S/C molar ratio on the reforming process

The effect of S/C molar ratio on the performance of the plasma reforming of toluene has been investigated to better understand the role of steam in this reaction. Fig.4 (a) presents the variation of toluene conversion and energy efficiency when changing the S/C molar ratio from 1 to 3.5 at a fixed toluene feed rate of 4.8 ml/h. Clearly, increasing the S/C molar ratio initially enhanced the toluene conversion of the plasma steam reforming of toluene and reached a maximum value of ~42.2% at an S/C molar ratio of 2-3, beyond which the toluene conversion gradually decreased to 38.3% at an S/C molar ratio of 3.5. Lim et al. also reported an optimal S/C molar ratio of 2-2.5 to achieve the maximum conversion of naphthalene and benzene in the conversion of light tars using a GAD [26]. The energy efficiency of the plasma process showed a similar evolution and reached the maximum (~27.3 g/kWh) at the S/C molar ratio of 2-3. The yield of gaseous products strongly depends on the S/C molar ratio with the optimal S/C molar ratio being 2-3. For instance, the highest yields of H₂ and CO were 30.4% and 35.1%, respectively, obtained at an S/C molar ratio of 2-3. However,

increasing the S/C molar ratio gradually decreased the yield of C_2H_2 from 12.8% to 5.3%. A higher S/C molar ratio could generate more OH radicals which participate in the oxidation of toluene and intermediates, thus reducing the chance of toluene ring cleavage by free electrons and N_2 excited species to release C_2H_2 . Trushkin et al also reported that an increase in flow humidity leads to a noticeable increase in the yield of CO and a suppression of acetylene yield [27]. Compared with major gas products H_2 , CO and C_2H_2 , only a small amount of C_2H_4 , C_2H_6 and C_3H_8 were formed in the plasma steam reforming of toluene with a total yield of no more than 1% under all experimental conditions.



(a)



(b)

Fig. 4 Effect of S/C molar ratio on (a) toluene conversion and energy efficiency; (b) yields of primary gaseous products (C_7H_8 feed rate: 4.8 ml/h; SEI: 0.19 kWh/m^3)

Clearly, humidity has a significant effect on toluene conversion in the plasma process. To better understand the role of S/C molar ratio on the reaction pathways in the plasma steam reforming of toluene, the effect of different S/C molar ratios on the relative intensity of three key radicals (CH, CN and OH) was investigated, as presented in Fig. 5. Clearly, increasing the S/C molar ratio from 1 to 3.5 significantly increased the relative intensity of OH. The presence of OH radicals in the plasma reaction opens a new route for toluene decomposition through step-wise oxidation of toluene and intermediates, resulting in an enhanced conversion and energy efficiency, as shown in Fig. 2. Meanwhile, the relative intensity of CN dropped significantly when increasing the S/C molar ratio. CN radicals could be produced from the reactions of N_2 with C_2 (R5). Fig. 4 shows that increasing the S/C molar ratio suppressed the formation of C_2 in the plasma reaction, which might also limit the formation of CN radicals. In addition, less carbon deposition was observed when adding steam into the plasma reforming of toluene, which might also reduce the production of CN as one possible route for CN formation could be the reaction between N and carbon (R8). The intensity of CH radical initially increased with the S/C molar ratio and reached a peak at an S/C ratio of 2.5, and then dropped with further increase of the S/C ratio. The evolution of the CH intensity with the S/C molar ratio is very similar to the effect of S/C ratio on the conversion of toluene (Fig. 4), which indicates that CH might be mainly produced from the dissociation of CH_3 and CH_2 by electrons and N_2 excited states, and closely associated with the decomposition of toluene in this reaction.

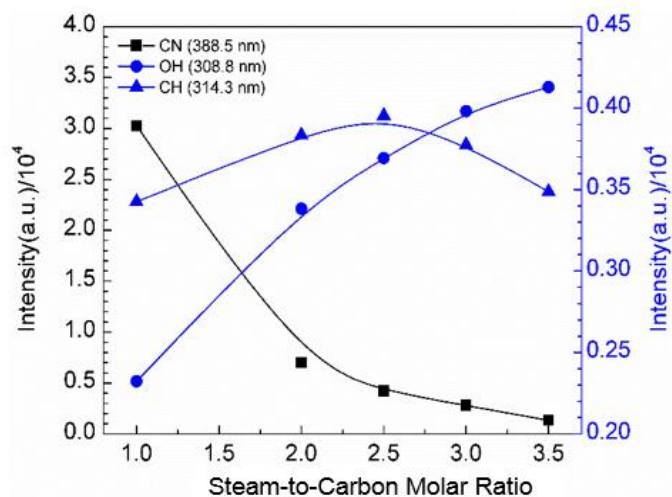
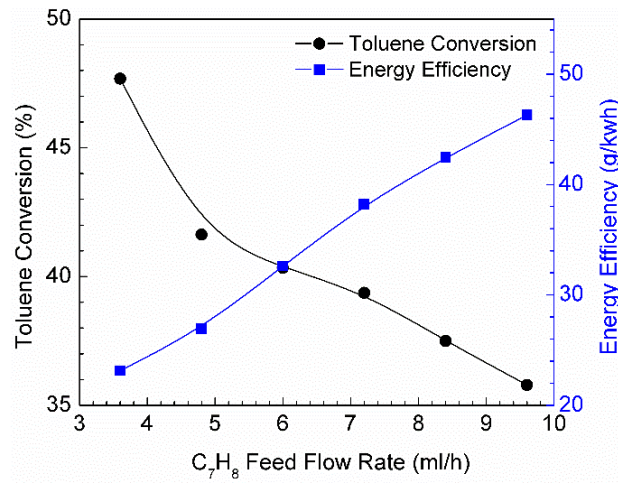


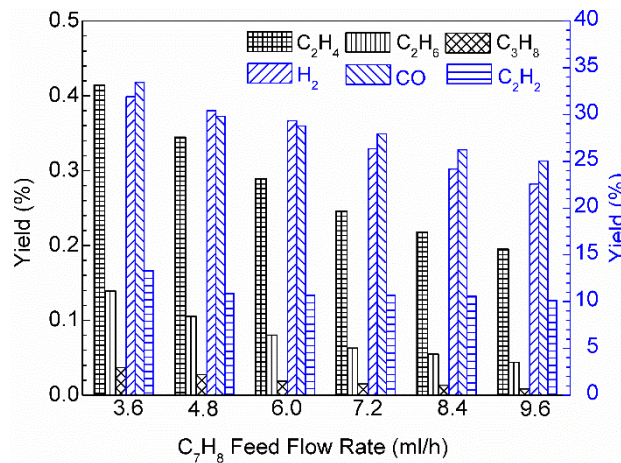
Fig.5 Optical emission intensity of three species in $N_2/H_2O/C_7H_8$ plasma as a function of water vapour amount (C_7H_8 feed rate: 4.8 ml/h; SEI: 0.19 kWh/m³).

3.3 Effect of toluene feed rate on the steam reforming process

Fig.6 (a) shows the effect of toluene feed rate on the toluene conversion and energy efficiency of the plasma process at a constant discharge power of 43.5 W. The conversion of toluene decreased from 47.7 % to 35.8 % when increasing the toluene feed rate from 3.6 to 9.6 ml/h, whereas the energy efficiency of the plasma process was doubled (from 23.1 to 46.3 g/kWh), which means more toluene was decomposed at a higher toluene feed rate. The yield of H_2 and CO followed the same tendency as the toluene conversion, and decreased from 31.9 % and 33.4 % to 22.6 % and 25 %, respectively, with the increase of toluene feed rate from 3.6 to 9.6 ml/h. C_2H_2 was found to be a major gas product with a maximum yield of 13.3 %, while the total yield of other hydrocarbons was lower than 1%.



(a)



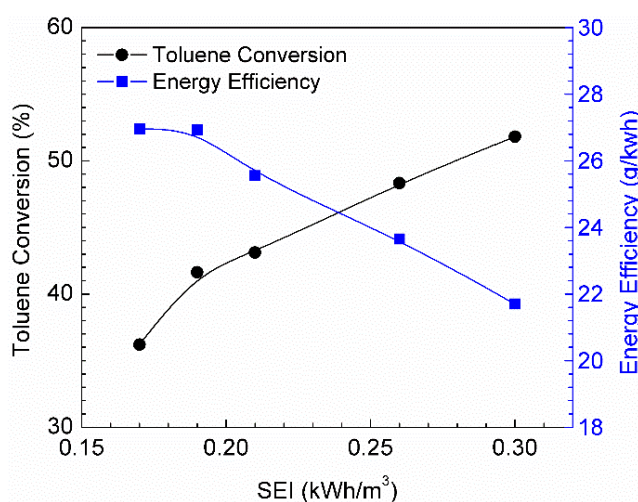
(b)

Fig. 6 Effect of toluene feed rate on: (a) toluene conversion and energy efficiency; (b) yields of main gaseous products (discharge power: 43.5 W; S/C=2)

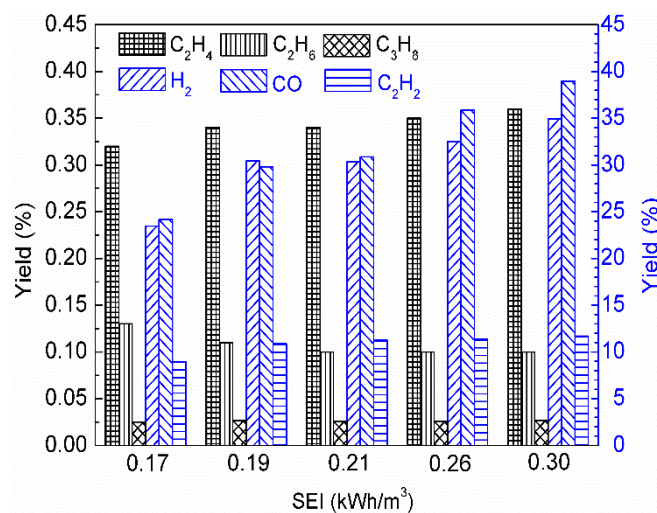
3.4. Effect of SEI on the reforming progress

SEI is one of the most important parameters affecting plasma chemical reactions as it is closely related to the power input to the plasma process. The influence of SEI on the reaction performance of the plasma toluene reforming is shown in Fig. 7. The SEI of the plasma is varied in the range of 0.17 - 0.30 kWh/m³ by changing the discharge power from 37 to 68 W at a constant total flow rate of 0.23 Nm³/h. The toluene conversion increased continuously up

to 51.8% at a SEI of 0.30 kWh/m³. A similar tendency was reported in tar conversion either using plasma alone or using plasma-catalysis [26, 28, 29]. Increasing SEI also enhanced the production of syngas. For instance, the yield of H₂ was enhanced by about 36 % when the SEI increased from 0.17 to 0.3 kWh/m³. Note that the yield of C₃ saturated hydrocarbon was almost independent of SEI in the tested range. Previous studies showed that increasing plasma power at a constant excitation frequency effectively enhances the electric field, electron energy and gas temperature in the discharge zone [14]. All of these properties may contribute in different ways to the enhanced toluene conversion and syngas production. In addition, increasing the discharge power produces more chemically reactive species (e.g. OH, N and N₂ excited states) which participate in the conversion of toluene and intermediates in the plasma reaction. The maximum energy efficiency of 27.0 g/kWh was obtained at the lowest SEI of 0.17 kWh/m³, which is greater than that obtained using a microwave plasma (4.52 g/kWh) [16] and a GAD plasma (20.9 g/kWh) in previous studies [21]. In addition, increasing SEI resulted in a reduction in energy efficiency of the plasma reaction, although the conversion of toluene was increased.



(a)



(b)

Fig. 7 Effect of SEI on (a) toluene conversion and energy efficiency; (b) yields of main gaseous products (toluene flow rate: 4.8 ml/h; S/C=2).

3.5 Comparison of process performance using different plasmas

Table 1 shows a comparison of the energy efficiency (E) and conversion efficiency (X) for the conversion of model tar compounds (toluene, benzene and naphthalene) using different non-thermal plasmas. It is clear that the energy efficiency (46.3 g/kWh) for the conversion of tar in this work is much higher than that of most of the other plasma processes. Notably, the energy efficiency of the process using gliding arc is significantly higher than that using DBD or corona discharge, which might be attributed to higher electron density in the gliding arc discharge. Our previous study showed that the electron density ($\sim 10^{23} \text{ m}^{-3}$) in the gliding arc discharge is several orders of magnitude higher than that in the DBD (10^{16} - 10^{19} m^{-3}) and corona discharge (10^{15} - 10^{19} m^{-3}) [14]. As shown in Table 1, very high toluene conversion efficiency (99%) can be achieved using the microwave plasma at an inlet toluene concentration of 4.2 g/Nm^3 . However, the corresponding energy efficiency of this process was only 4.5 g/kWh, which is significantly lower than that obtained in this work. A balance between tar conversion and energy efficiency in the plasma process is significantly important

for the development and deployment of an efficient and cost-effective plasma process for tar removal.

Further enhancement in the conversion and energy efficiency of tar reforming using a gliding arc plasma can be expected from the optimization of reactor geometry, power supply and plasma operating parameters. For instance, developing a rotating gliding arc reformer with a 3-dimensional configuration can ensure that all the reactants pass through the plasma area, which can increase the reaction time of the reactants in the plasma and significantly enhance the reaction performance [14, 22]. Furthermore, the reaction conditions, such as the power source and electrode material, as well as the types and concentration of the carrier gas, can be better controlled to optimize the performance of gliding arc plasmas. Previous studies have demonstrated that the waveform of applied voltage can not only control the applied electric field, which affects the density of the energetic electrons and the reactive species generated, but can also improve the energy transfer with subsequent improvement of the energy efficiency of the plasma process [30]. This conclusion was supported by a simulation study, which showed that the energy efficiency of a plasma reactor can be enhanced by a factor of 4 when using rectangular pulse instead of a sinusoidal voltage [31]. The combination of plasma with highly active catalysts might provide a promising solution to generate a synergistic effect, which can further enhance the reaction productivity and energy efficiency of the plasma process.

Table 1 Comparison of reaction performance of tar removal by different plasmas

Process	Tar	Working Gas	Tar Content (g/Nm ³)	Q (m ³ /h)	SEI (kWh/m ³)	X (%)	E (g/kWh)	Ref
AC GAD	C ₆ H ₆	Humid N ₂	4.3	1.0	0.17	82.6	20.9	[21]
Microwave Torch	C ₇ H ₈	20% Ar+N ₂	4.2	1.07	0.93	99.0	4.5	[16]
DC GAD	C ₁₀ H ₈	O ₂	1.3	0.4	0.47	92.0	3.6	[32]
3-electrode GAD	C ₁₀ H ₈	Humid N ₂	14.3	1.1	1	79.0	47	[22]
DBD with MnO ₂ /γ-Al ₂ O ₃	C ₇ H ₈	Dry Air	1.0	0.12	0.01	98.0	0.7	[33]
Positive Corona	C ₇ H ₈	Dry Air	0.8	0.02	0.19	15.0	2.5	[34]
AC GAD	C ₇ H ₈	Humid N ₂	23.5	0.23	0.19	35.8	46.3	This work

4. Reaction mechanisms

To understand the reaction mechanisms and pathways in the plasma steam reforming of toluene, liquid-phase end-products were qualitatively analyzed using GC-MS, as shown in Fig. 8 and Table 2. In this reaction, benzonitrile, benzene (butoxymethyl), benzenpropanenitrile and benzene were identified as the major liquid compound. The production of these N-containing organic compounds suggests that NH_x (x=1 and 2) and CN radicals participate in the reactions through their recombination with intermediates from toluene decomposition. In addition, naphthalene was clearly identified as a dominant polycyclic product, which might be formed from the combination of cyclopentadienyl radicals [37]. Remarkably, linear product panaxynone was also detected, resulting from the cleavage of a toluene ring followed by the recombination or hydrogenation of the intermediates, including methyl, bi-radical HC=CH and acetylene.

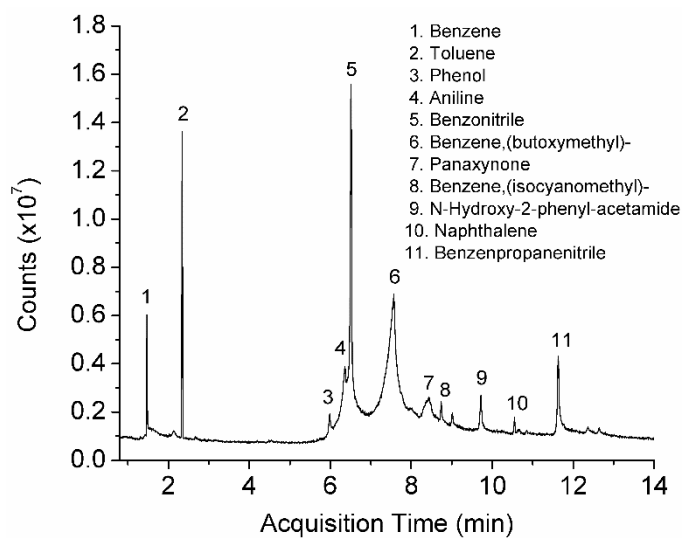
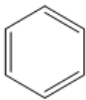
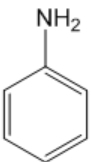
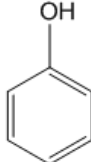
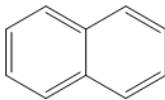
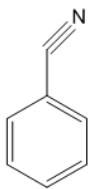
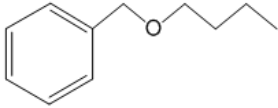
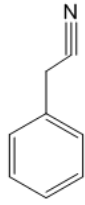
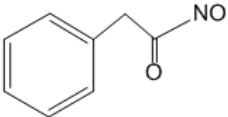
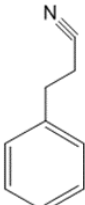
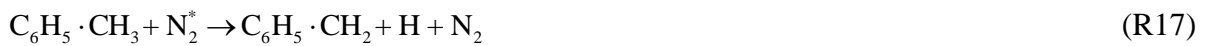


Fig. 8 GC/MS analysis of liquid sample after plasma steam reforming of toluene (toluene flow rate: 4.8 ml/h; S/C=2; SEI: 0.19 kWh/m³).

Table 2 Products identified in liquid sample by GC-MS

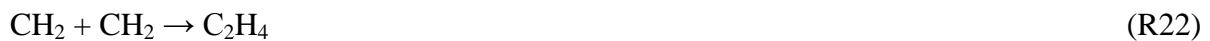
			
Benzene	Aniline	Phenol	Naphthalene
			
Benzonitrile	Benzene (butoxymethyl)	Benzene (isocyanomethyl)	
			
N-hydroxy-2-phenyl-acetamide	Benzenpropanenitrile		

The destruction of low concentration toluene in the nitrogen GAD can be initialized through two major reaction pathways: H-abstraction of the methyl group and breaking the benzene ring through reactions induced by energetic electrons and N₂ excited states such as N₂ (A³) and N₂ (a¹), shown in R13-R20.



Previous experimental and modelling studies showed the importance of N₂ excited states in the destruction of low concentration gas pollutants in nitrogen or air plasmas [38, 39]. Trushkin et al. developed a kinetic model to understand the decomposition of toluene (100-400 ppm) in a nitrogen pulsed discharge. Their results showed that toluene is mainly decomposed via its reactions with N₂ excited species, such as N₂ (A³) and N₂ (a¹) [40]. Yu et al. demonstrated that the destruction of naphthalene (20-140 ppm) in a gliding arc reactor is mainly initialized through its reactions with nitrogen excited states, while the electron impact reactions play a weak role in the decomposition of naphthalene. This can be evidenced by a lower naphthalene decomposition in the Ar/O₂ gliding arc compared to that using the N₂/O₂ GAD [32].

In the plasma steam reforming of toluene, the produced OH radicals from steam can oxidize toluene and intermediates, opening a new reaction pathway for the destruction of toluene, resulting in the enhanced conversion and energy efficiency of the plasma process. H₂, CO and C₂H₂ were identified as the major gaseous products in the plasma steam reforming of toluene in this study. Hydrogen can be formed through the recombination of two H atoms, which are more likely generated from a methyl group (R13 and R17) than from a benzene ring (R14 and R18) as the dissociation energy of C-H bonds (3.7 eV) in the methyl group are the weakest bonds in the toluene molecules [35]. The toluene ring cleavage by free electrons or N₂ excited species to form C₂H₂ and C₅H₆ could be the major route for the production of acetylene in this process (R16 and R20) due to the high yield of C₂H₂. C₂H₄, C₂H₆ and C₃H₈ are generally formed through the neutral-neutral recombination of radicals (e.g. CH₃, CH₂, C₂H₅, etc), as shown in R21-R23. However, only trace amounts of these gaseous products were detected in the plasma reforming of toluene, which suggests the following reactions are unimportant.



The recombination of CH₃ with H can form CH₄ (R24). However, no CH₄ was detected in the plasma conversion of toluene with or without steam, suggesting that this reaction (R24) is ineligible.



The possible mechanism of toluene decomposition is schematically shown in Fig. 9. The dissociation energy of the C-H bond in methyl is 3.7 eV, which is smaller than that of the C-

H bond in the aromatic ring (4.3 eV), the C-C bond between methyl group and aromatic ring (4.4 eV), the C-C bond in the aromatic ring (5.0-5.3eV) and the C=C bond in the aromatic ring (5.5 eV) [41]. Therefore, the primary pathway of toluene decomposition could be the H-abstraction from the methyl group by nitrogen excited species or energetic electrons [36]. The generated benzyl radicals (I) from the H-abstraction of methyl could react with OH to form benzaldehyde (II), which can be further oxidized to form benzoic acid. These aromatic intermediates can also be decomposed through collisions with energetic electrons and reactive species to produce phenyl radicals (III) [42]. In addition, C-C bonds between methyl and benzene ring can be easily broken by nitrogen excited species and energetic electrons, generating phenyl radicals. As shown in Fig. 9, phenol radicals could react with H, OH, NH₂ and CN radicals, forming benzene (IV), phenol (V), aniline (VI) and benzonitrile (VII), respectively, all of which were identified by GC-MS after the plasma reaction. The recombination of methyl and benzyl radicals produces ethylbenzene, which is followed by further reaction with CN to form benzene (isocyanomethyl) (VIII). Blin-Simiand et al. reported that the possibility of the reaction [43]between CN and phenyl was higher than that between CN and methyl-phenyl in the destruction of toluene using a DBD [44]. Toluene can also be ruptured by the dissociation of C-C bonds of the aromatic ring with a dissociation energy of 6.0 eV, resulting in the direct cleavage of the aromatic ring to produce bi-radical HC=CH (IX) and methyl-cyclobutadiene (X) [44]. The other route of toluene conversion might be induced by the oxidation of the aromatic ring, producing hydroxycyclohexadienyl type peroxy radicals (XI) [23], which has been confirmed in the previous modelling and experimental studies [23, 42, 43, 45]. This unstable reactive compound can form a peroxide bridge radical, which is a precursor for both the carbonyl and epoxide routes. The carbonyl reaction route opens a ring of toluene via a series of oxidation steps by O/OH radicals to form a relatively stable epoxide (XII) [23]. In addition, the epoxide radicals can also be

decomposed by energetic electrons or reactive species, consequently forming syngas and H₂O.

The possible reactions could be the scission of 2, 3-carbon or 1, 2-carbon bond of epoxide, leading to the formation of oxalic acid (XIII), formic acid (XIV), and eventually producing CO and H₂.

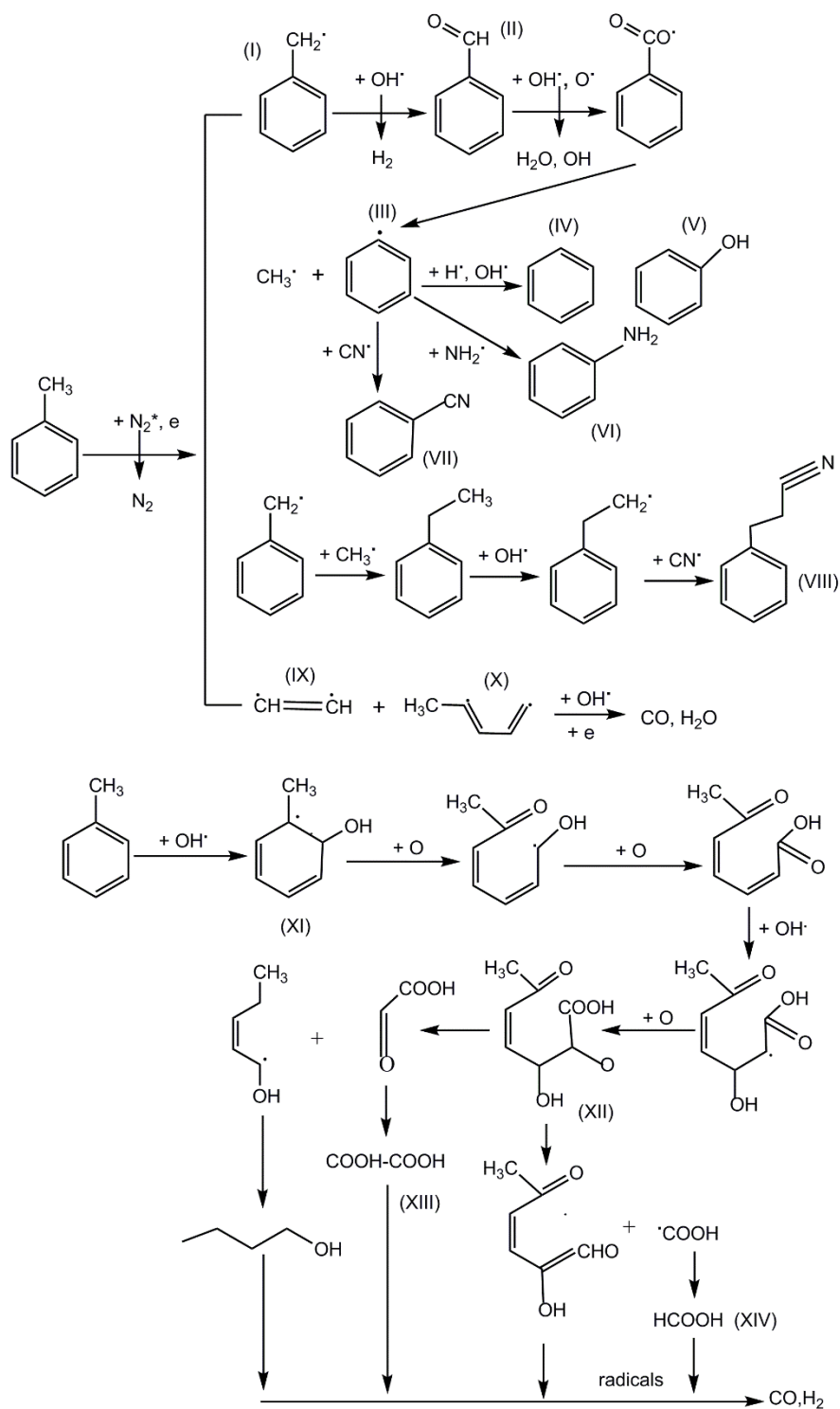


Fig. 9 Possible reaction pathways for toluene destruction

5. Conclusion

The conversion of toluene as a model tar compound from biomass gasification was carried out in an AC gliding arc discharge reactor at atmosphere pressure. Adding steam to the plasma toluene reaction significantly enhanced the conversion of toluene and the energy efficiency of the plasma process due to the formation of OH radicals which open a new reaction route for the decomposition of toluene through a stepwise oxidation of toluene and intermediates. The effect of different process parameters on the performance of the plasma steam reforming of toluene was also investigated in terms of the toluene conversion, yield of products and energy efficiency of the plasma process. The performance of the plasma process strongly depends on the S/C molar ratio with the optimal S/C molar ratio being 2-3. The maximum toluene conversion of 51.8% was achieved at an optimal S/C molar ratio of 2, a toluene feed flow rate of 4.8 ml/h and a SEI of 0.3 kWh/m³, while the energy efficiency of the plasma process reached a maximum (~46.3 g/kWh) at the same S/C molar ratio, but a higher toluene feed flow rate (9.6 ml/h) and a lower SEI (0.19 kWh/m³). H₂, CO and C₂H₂ were identified as the major gas products, while a trace amount of hydrocarbons (C₂H₄, C₂H₆ and C₃H₈) with a total yield of less than 1% were also detected in the effluent. The S/C molar ratio also has a significant influence on the yield of gaseous products. The maximum syngas production (73.9% gas yield) was achieved at the same condition as that for the maximum toluene conversion. However, increasing the S/C molar ratio gradually decreased the yield of C₂H₂ from 12.8% to 5.3% at a toluene feed flow rate of 4.8 ml/h and a SEI of 0.19 kWh/m³. Higher S/C molar ratio could generate more OH radicals for the stepwise oxidation of toluene and intermediates, reducing the chance of toluene ring cleavage by free electrons and N₂ excited species to release C₂H₂. In addition, a small amount of liquid by-products were also collected after the plasma steam reforming of toluene. The possible mechanisms and reaction

pathways in the plasma conversion of toluene have been proposed and discussed in detail based on the analysis of the gas and liquid samples and the formation of reactive species (e.g. CH, OH, CN and NH) using OES under different experimental conditions.

Acknowledgement

The support of this work by the EPSRC SUPERGEN Bioenergy Challenge II Programme (EP/M013162/1) is gratefully acknowledged.

Reference

- [1] H. Hofbauer, G. Veronik, T. Fleck, R. Rauch, H. Mackinger, E. Fercher, *The FICFB — Gasification Process*, Springer Netherlands 1997.
- [2] S. Consonni, F. Vigano, Waste gasification vs. conventional Waste-to-Energy: a comparative evaluation of two commercial technologies, *Waste Manag* 32 (2012) 653-666.
- [3] S. Anis, Z.A. Zainal, Tar reduction in biomass producer gas via mechanical, catalytic and thermal methods: A review, *Renewable and Sustainable Energy Reviews* 15 (2011) 2355-2377.
- [4] Y. Richardson, J. Blin, A. Julbe, A short overview on purification and conditioning of syngas produced by biomass gasification: Catalytic strategies, process intensification and new concepts, *Progress in Energy and Combustion Science* 38 (2012) 765-781.
- [5] M. Ni, D.Y.C. Leung, M.K.H. Leung, K. Sumathy, An overview of hydrogen production from biomass, *Fuel Process Technol* 87 (2006) 461-472.
- [6] L. Fagbemi, L. Khezami, R. Capart, Pyrolysis products from different biomasses: application to the thermal cracking of tar, *Appl Energy* 69 (2001) 293-306.
- [7] B.S. Pathak, D.V. Kapatel, P.R. Bhoi, A.M. Sharma, D.K. Vyas, Design and development of sand bed filter for upgrading producer gas to IC engine quality fuel, *International Energy Journal* 8 (2007) 15-20.
- [8] A.G. Bhave, D.K. Vyas, J.B. Patel, A wet packed bed scrubber-based producer gas cooling-cleaning system, *Renew Energ* 33 (2008) 1716-1720.
- [9] H. Noichi, A. Uddin, E. Sasaoka, Steam reforming of naphthalene as model biomass tar over iron–aluminum and iron–zirconium oxide catalysts, *Fuel Process Technol* 91 (2010) 1609-1616.
- [10] M. Kong, J.H. Fei, S.A. Wang, W. Lu, X.M. Zheng, Influence of supports on catalytic behavior of nickel catalysts in carbon dioxide reforming of toluene as a model compound of tar from biomass gasification, *Bioresource Technology* 102 (2011) 2004-2008.
- [11] R.Q. Zhang, H.J. Wang, X.X. Hou, Catalytic reforming of toluene as tar model compound: Effect of Ce and Ce-Mg promoter using Ni/olivine catalyst, *Chemosphere* 97 (2014) 40-46.
- [12] D. Świerczyński, S. Libs, C. Courson, A. Kiennemann, Steam reforming of tar from a biomass gasification process over Ni/olivine catalyst using toluene as a model compound, *Applied Catalysis B: Environmental* 74 (2007) 211-222.
- [13] F. Odeyemi, A. Rabinovich, A. Fridman, Gliding Arc Plasma-Stimulated Conversion of Pyrogas into Synthesis Gas, *IEEE Transactions on Plasma Science* 40 (2012) 1124-1130.
- [14] X. Tu, J.C. Whitehead, Plasma dry reforming of methane in an atmospheric pressure AC gliding arc discharge: Co-generation of syngas and carbon nanomaterials, *Int J Hydrogen Energ* 39 (2014) 9658-9669.
- [15] S.Y. Liu, D.H. Mei, Z. Shen, X. Tu, Nonoxidative Conversion of Methane in a Dielectric Barrier Discharge Reactor: Prediction of Reaction Performance Based on Neural Network Model, *The Journal of Physical Chemistry C* 118 (2014) 10686-10693.
- [16] R.M. Elliott, M.F.M. Nogueira, A.S. Silva Sobrinho, B.A.P. Couto, H.S. Maciel, P.T. Lacava, Tar Reforming under a Microwave Plasma Torch, *Energy Fuel* 27 (2013) 1174-1181.
- [17] S.A. Nair, A.J.M. Pemen, K. Yan, F.M. van Gompel, H.E.M. van Leuken, E.J.M. van Heesch, K.J. Ptasiński, A.A.H. Drinkenburg, Tar removal from biomass-derived fuel gas by pulsed corona discharges, *Fuel Process Technol* 84 (2003) 161-173.
- [18] A. Fridman, S. Nester, L.A. Kennedy, A. Saveliev, O. Mutaf-Yardimci, Gliding arc gas discharge, *Prog. Energy Combust. Sci.* 25 (1999) 211-231.
- [19] N. Tippayawong, P. Inthasan, Investigation of Light Tar Cracking in a Gliding Arc Plasma System, *Int J Chem React Eng* 8 (2010).
- [20] D. Swierczyński, C. Courson, A. Kiennemann, Study of steam reforming of toluene used as model compound of tar produced by biomass gasification, *Chem Eng Process* 47 (2008) 508-513.
- [21] Y.N. Chun, S.C. Kim, K. Yoshikawa, Decomposition of benzene as a surrogate tar in a gliding Arc plasma, *Environmental Progress & Sustainable Energy* 32 (2013) 837-845.

- [22] Y.C. Yang, Y.N. Chun, Naphthalene destruction performance from tar model compound using a gliding arc plasma reformer, *Korean J Chem Eng* 28 (2011) 539-543.
- [23] J. Van Durme, J. Dewulf, W. Sysmans, C. Leys, H. Van Langenhove, Abatement and degradation pathways of toluene in indoor air by positive corona discharge, *Chemosphere* 68 (2007) 1821-1829.
- [24] J.A. Manion, R.E. Huie, R.D. Levin, D.R. Burgess Jr., V.L. Orkin, W. Tsang, NIST Chemical Kinetics Database, NIST Standard Reference Database 17, Gaithersburg, Maryland, 2015.
- [25] H. Zhang, F. Zhu, X. Li, K. Cen, C. Du, X. Tu, Rotating Gliding Arc Assisted Water Splitting in Atmospheric Nitrogen, *Plasma Chem Plasma P* 36 (2016) 813-834.
- [26] M.-S. Lim, Y.-N. Chun, Light Tar Decomposition of Product Pyrolysis Gas from Sewage Sludge in a Gliding Arc Plasma Reformer, *Environmental Engineering Research* 17 (2012) 89-94.
- [27] A.N. Trushkin, I.V. Kochetov, Simulation of toluene decomposition in a pulse-periodic discharge operating in a mixture of molecular nitrogen and oxygen, *Plasma Phys Rep+* 38 (2012) 407-431.
- [28] T. Nunnally, A. Tsangaris, A. Rabinovich, G. Nirenberg, I. Chernets, A. Fridman, Gliding arc plasma oxidative steam reforming of a simulated syngas containing naphthalene and toluene, *Int J Hydrogen Energ* 39 (2014) 11976-11989.
- [29] H. Ge, D.X. Hu, X.G. Li, Y. Tian, Z.B. Chen, Y.M. Zhu, Removal of low-concentration benzene in indoor air with plasma-MnO₂ catalysis system, *J Electrostat* 76 (2015) 216-221.
- [30] A.A. Abdelaziz, T. Seto, M. Abdel-Salam, T. Ishijima, Y. Otani, Influence of applied voltage waveforms on the performance of surface dielectric barrier discharge reactor for decomposition of naphthalene, *Journal of Physics D: Applied Physics* 48 (2015) 195201.
- [31] T. Martens, A. Bogaerts, J. van Dijk, Pulse shape influence on the atmospheric barrier discharge, *Appl Phys Lett* 96 (2010) 131503.
- [32] L. Yu, X. Li, X. Tu, Y. Wang, S. Lu, J. Yan, Decomposition of naphthalene by dc gliding arc gas discharge, *J Phys Chem A* 114 (2010) 360-368.
- [33] T. Zhu, J. Li, W. Liang, Y. Jin, Synergistic effect of catalyst for oxidation removal of toluene, *J Hazard Mater* 165 (2009) 1258-1260.
- [34] W. Mista, R. Kacprzyk, Decomposition of toluene using non-thermal plasma reactor at room temperature, *Catal Today* 137 (2008) 345-349.
- [35] F.S. Zhu, X.D. Li, H. Zhang, A.J. Wu, J.H. Yan, M.J. Ni, H.W. Zhang, A. Buekens, Destruction of toluene by rotating gliding arc discharge, *Fuel* 176 (2016) 78-85.
- [36] H. Huang, D. Ye, D.Y.C. Leung, F. Feng, X. Guan, Byproducts and pathways of toluene destruction via plasma-catalysis, *Journal of Molecular Catalysis A: Chemical* 336 (2011) 87-93.
- [37] H.R. Zhang, E.G. Eddings, A.F. Sarofim, Modeling benzene and naphthalene formation in a premixed propylene flame, Fall Technical Meeting of the Western States Section of the Combustion Institute 2005, Western States Section/Combustion Institute, United States, Stanford, 2005, pp. 657-675.
- [38] R. Aerts, X. Tu, C. De Bie, J.C. Whitehead, A. Bogaerts, An Investigation into the Dominant Reactions for Ethylene Destruction in Non-Thermal Atmospheric Plasmas, *Plasma Processes and Polymers* 9 (2012) 994-1000.
- [39] X. Zhu, X. Gao, R. Qin, Y. Zeng, R. Qu, C. Zheng, X. Tu, Plasma-catalytic removal of formaldehyde over Cu-Ce catalysts in a dielectric barrier discharge reactor, *Applied Catalysis B-Environmental* 170 (2015) 293-300.
- [40] A.N. Trushkin, M.E. Grushin, I.V. Kochetov, N.I. Trushkin, Y.S. Akishev, Decomposition of toluene in a steady-state atmospheric-pressure glow discharge, *Plasma Phys Rep+* 39 (2013) 167-182.
- [41] H. Kohno, A.A. Berezin, C. Jen-Shih, M. Tamura, T. Yamamoto, A. Shibuya, S. Honda, Destruction of volatile organic compounds used in a semiconductor industry by a capillary tube discharge reactor, *IEEE Trans. Ind. Appl* 34 (1998) 953-966.
- [42] C.M. Du, J.H. Yan, B. Cheron, Decomposition of toluene in a gliding arc discharge plasma reactor, *Plasma Sources Sci T* 16 (2007) 791-797.
- [43] L.J. Bartolotti, E.O. Edney, Density functional theory derived intermediates from the OH initiated atmospheric oxidation of toluene, *Chem. Phys. Lett.* 245 (1995) 119-122.

- [44] N. Blin-Simiand, F. Jorand, L. Magne, S. Pasquiers, C. Postel, J.R. Vacher, Plasma reactivity and plasma-surface interactions during treatment of toluene by a dielectric barrier discharge, *Plasma Chem Plasma P* 28 (2008) 429-466.
- [45] S.Y. Lu, X.M. Sun, X.D. Li, J.H. Yan, C.M. Du, Decomposition of Toluene in a Rotating Glidarc Discharge Reactor, *IEEE Trans. Plasma Sci.* 40 (2012) 2151-2156.